Journal of Research of the National Bureau of Standards Vol. 61, No. 4, October 1958 Research Paper 2900

Pseudoternary System Calcium Oxide-Monocalcium Aluminate ($CaO \cdot Al_2O_3$)-Dicalcium Ferrite ($2CaO \cdot Fe_2O_3$)

Terry F. Newkirk [1, 2] and R. D. Thwaite [2]

The system CaO-$CaO \cdot Al_2O_3$-$2CaO \cdot Fe_2O_3$ is of importance to portland cement chemistry because it provides information on the composition of the iron-bearing phase in cement clinker.

Iron-bearing solid solutions in the system were found to exist as a continuous narrow band extending from $2CaO \cdot Fe_2O_3$ to $6.45CaO \cdot 2.31Al_2O_3 \cdot F_2O_3$. Additional tie lines were established to show the composition of the iron-bearing solid solution phase (Fss) and liquid phases during the course of crystallization of mixtures within the system. Isotherms have been located for the regions of principal interest. Compatibility relations differ somewhat from those reported by previous investigators. The composition of the iron-bearing phase in equilibrium with CaO and $3CaO \cdot Al_2O_3$ at the ternary invariant point proved to be lower in Fe_2O_3 than that reported by Swayze. Other results are in general agreement with the work of Swayze and of Yamauchi.

1. Introduction

In its effect on the constitution of portland cement clinker, Fe_2O_3 is next in importance to the three principal components CaO, Al_2O_3, and SiO_2. Le Chatelier [1][3] postulated the existence in portland cement clinker of a ternary compound of calcium, aluminum, and ferric oxides having a possible formula $3CaO \cdot Al_2O_3 \cdot Fe_2O_3$. In their pioneering work on the system CaO-$CaO \cdot Al_2O_3$-$CaO \cdot Fe_2O_3$, Hansen, Brownmiller, and Bogue [2] discovered a continuous series of solid solutions between the compound $2CaO \cdot Fe_2O_3$ and what appeared to be a compound, $4CaO \cdot Al_2O_3 \cdot Fe_2O_3$. The latter phase ($Al_2O_3/Fe_2O_3$ weight ratio 0.64) was believed to constitute the end of the solid-solution series. Commercial portland cements are ordinarily of higher Al_2O_3/Fe_2O_3 ratios than 0.64. The existence of a series of solid solutions in the region of lower ratios was, therefore, not of primary interest to portland cement chemists at that time, because it appeared that the iron-bearing solid solutions would rarely, if ever, be found in clinker.

Based on this earlier work, Lea and Parker [3] investigated the system CaO-$2CaO \cdot SiO_2$-$5CaO \cdot 3Al_2O_3$[4]-$4CaO \cdot Al_2O_3 \cdot Fe_2O_3$, treating all of the calcium aluminoferrite phases as having the composition $4CaO \cdot Al_2O_3 \cdot Fe_2O_3$.

Further work on the ternary system CaO-$CaO \cdot Al_2O_3$-$4CaO \cdot Al_2O_3 \cdot Fe_2O_3$ was done by McMurdie [6] who studied in detail the extent of solid solutions within that system. His compositions and two of the temperatures for the ternary invariant points differ from those reported [2] earlier. Certain discrepancies noted between the calculated and observed compositions of the iron-bearing phase in some commercial clinkers led to independent investigations by Yamauchi [7] and by Swayze [8] of the system CaO-$5CaO \cdot 3Al_2O_3$-$2CaO \cdot Fe_2O_3$ and by Swayze [9] of the quaternary system CaO-$5CaO \cdot 3Al_2O_3$-$2CaO \cdot Fe_2O_3$-$2CaO \cdot SiO_2$ and of the same system as modified by 5 percent of MgO. These investigators discovered that the solid solution between $2CaO \cdot Fe_2O_3$ and a hypothetical $2CaO \cdot Al_2O_3$ extended beyond $4CaO \cdot Al_2O_3 \cdot Fe_2O_3$, in which the molar Al_2O_3/Fe_2O_3 ratio is unity. This discovery was of importance to the cement industry because it showed that the composition of the principal iron-bearing phase in most commercial clinkers is not fixed but may vary with the chemical composition of the clinker. Changes in the compositions of these iron-bearing solid solutions can affect significantly the constitution and properties of the clinker. Swayze [8, 9] reported that the solid solutions of interest are confined to the pseudoternary system CaO-$5CaO \cdot 3Al_2O_3$-$2CaO \cdot Fe_2O_3$. His diagram for the ternary system differed in a number of respects from those of the earlier investigators.

Although the extension of the iron-bearing solid-solution series in the ternary system to higher Al_2O_3/Fe_2O_3 ratios than $4CaO \cdot Al_2O_3 \cdot Fe_2O_3$ has been confirmed by several investigators, there is some disagreement among them as to the limits of this series. Swayze placed the high-Al_2O_3 limit at the composition $6CaO \cdot 2Al_2O_3 \cdot Fe_2O_3$ (molar Al_2O_3/Fe_2O_3 ratio of 2.0) whereas Yamauchi [7] and Malquori and Cirilli [10] placed it at a ratio of 2.2 and 2.3, respectively.

Solid solution was pictured by Swayze as being limited to a straight line extending from $2CaO \cdot Fe_2O_3$ to the composition $6\,Ca\,O \cdot 2Al_2O_3 \cdot Fe_2O_3$ in the ternary system. Yamauchi referred to the solid solution series as being confined to a "swelled straight line." The composition $4CaO \cdot Al_2O_3 \cdot Fe_2O_3$ is a solid solution on this line [7, 10]. Some solid solution departing from the line is also indicated in the data of McMurdie [6] who noted that $4CaO \cdot Al_2O_3 \cdot Fe_2O_3$ can

---

[1] Present address, General Electric Company, Power Tube Department, Schenectady, N. Y.

[2] Research Associate, Portland Cement Association Fellowship, National Bureau of Standards.

[3] Figures in brackets indicate the literature references at the end of this paper.

[4] Studies by Büssem and Eitel [4], and by Thorvaldson and Schneider [5], indicate that the correct formula for this compound is $12CaO \cdot 7Al_2O_3$. The latter formula is used in the present work except in references to the work of earlier authors.

take into solution up to 5 percent of $3CaO{\cdot}Al_2O_3$, $5CaO{\cdot}3Al_2O_3$, or $CaO{\cdot}Al_2O_3$.

Because the composition of the iron-bearing phase is variable, it is necessary for the investigator to depict on the phase diagram the changing composition of these crystals as crystallization (or melting) proceeds by means of tie lines or conodes. Two tie lines were given by Swayze in each of the diagrams representing the ternary, quaternary, and quinary systems. The number is not sufficient, however, to permit one to follow the course of crystallization within each system.

The present study was undertaken in order to reconcile differences in published data on the ternary system. It also has the purpose of obtaining additional information on the system, especially the establishment of a sufficient number of tie lines to permit computation of the approximate composition of the calcium aluminoferrite phase throughout the crystallization of mixtures within the system. This information has an important bearing on the constitution of portland cement.

2. Experimental Methods

2.1. Preparation of Mixtures

All compositions were synthesized from reagent grade calcium carbonate S. L. (low-alkali type), Fe_2O_3, and Linde type-B alumina (99.9% Al_2O_3). These materials were dried and then weighed in the correct amounts to give 10-g samples on ignition. After an initial mixing for several hours in glass jars, the mixtures were ground in an alumina mortar to pass a No. 325 sieve. Each mixture was heated for three periods of at least 2 hr in the range 1,100° to 1,310° C before being studied. Following each burn, the sample was ground, screened, and remixed. Composition gradients within the individual crystals, because of changes in the liquid composition during crystallization, were unlikely because the temperature of first liquid formation for nearly all mixtures studied was above 1,310°. The exceptions, five mixtures with compositions in the $CaO{\cdot}Fe_2O_3$ compatibility regions, were heated 15 hr or more at 1,180° C to insure homogeneity. These mixtures were used for quenching experiments and for differential thermal analysis. Further heat treatment was given selected compositions prior to examination by X-ray diffraction methods.

2.2. Temperature Measurement and Control

Temperatures in the furnace were measured with a platinum–platinum-10%-rhodium thermocouple calibrated at melting points defined as follows: $CaMgSi_2O_6$, 1,392° C and $BaO{\cdot}2SiO_2$, 1,418° C. The furnace was maintained at constant temperature within ±0.5° C by means of a controller of the type developed by Mauer [11].

2.3. Methods of Investigation

Phase relations in this system were investigated by differential thermal analysis (DTA) and the standard quenching technique. The DTA studies made use of a pellet method [12] developed in the Fellowship laboratory. In the quenching technique, presintered mixtures of oxides were held in platinum envelopes at constant temperature for 2 hr until equilibrium was reached between solid and liquid phases, and then quenched in water. The identification of phases was based on the results of microscopic examinations and X-ray powder diffraction patterns made with a Philips high-angle diffractometer using $CuK\alpha$ radiation.

For studying final products of crystallization, small quantities of 17 glasses with compositions in the vicinity of the iron-bearing solid solution region, and near invariant points, were collected by quenching from above the liquidus. After devitrification in platinum capsules at 1,300° C for approximately 40 hr, the charges were removed from the furnace and mixed by grinding in a boron carbide mortar. This procedure was used to insure attaining equilibrium among the solid phases. A portion of each sample was then mixed with 5 percent by weight of pure tungsten powder as an internal standard prior to X-ray powder diffraction study. The diffraction patterns showed that all samples were well crystallized as a result of their heat treatment. The important portions of each pattern were scanned at a speed of 1/8°/min over the range 15° to 110° (2θ) using a 0.003-in. receiving slit, and a time constant that was small as compared with the time width [13] of the slit.

Tie lines in the system were determined by microscopic study and X-ray powder patterns of selected mixtures. Chosen compositions in the primary-phase region for the calcium aluminoferrite solid solution (Fss) were quenched at a temperature about 1° C below that at which the secondary crystalline phase appears, after being held long enough to reach equilibrium. By measuring d_{hkl} for a series of peaks found in the patterns, and correlating these with d_{hkl} values determined for the solid-solution series, the composition of the solid solution in equilibrium with the liquid and the secondary phase was determined. The tie line through points in the phase diagram representing the original mixture and the solid-solution phase intersects the boundary of the Fss primary-phase region at the liquidus temperature corresponding to the appearance of the secondary phase in crystallization of the original mixture.

3. Results and Discussion

3.1. General Information on the System

The phase diagram for the condensed ternary system $CaO\text{-}CaO{\cdot}Al_2O_3\text{-}2CaO{\cdot}Fe_2O_3$ developed in the present investigation appears as figure 1. The diagram contains a considerable amount of new information on tie lines, isotherms, compatibility regions, and the extent of the calcium aluminoferrite solid solutions in the system. The binary invariant points for $CaO\text{-}C_3A$, $C_3A\text{-}C_{12}A_7$, and $C_{12}A_7\text{-}CA$ were determined by Rankin and Wright [15], and that for $CaO\text{-}C_2F$ by Swayze [8]. Experimental data on which the diagram is based are given in table 1.

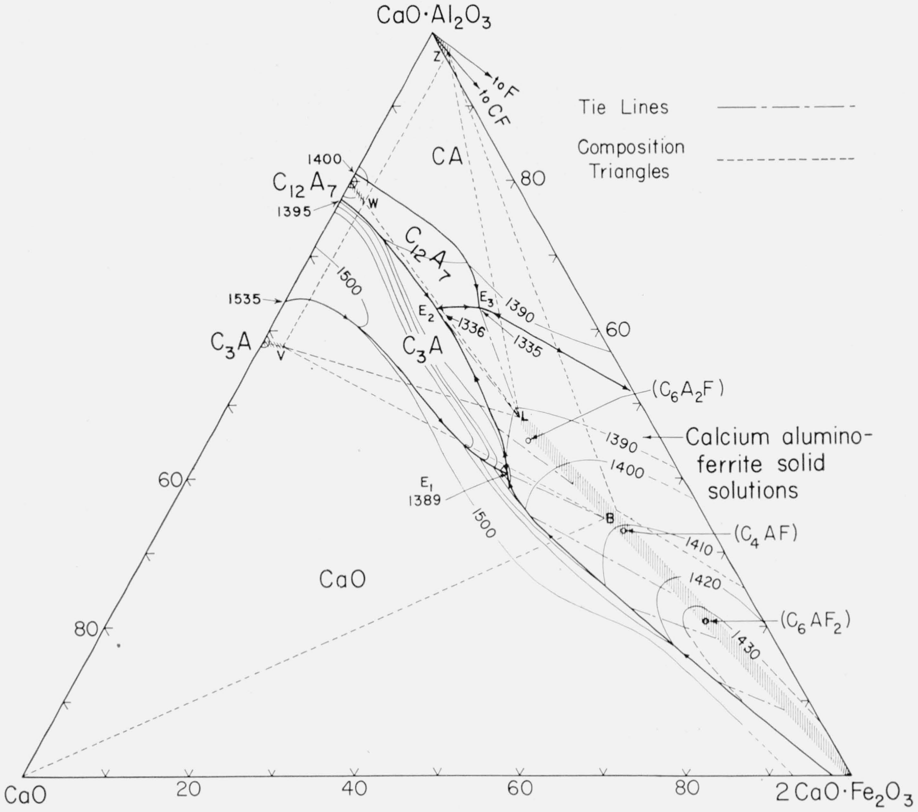

FIGURE 1. *Equilibrium diagram of the pseudo-ternary system* CaO-CaO·Al_2O_3-2CaO·Fe_2O_3 *showing isotherms, tie lines, and the fields of the primary crystalline phases.*

TABLE 1. *Quenching and DTA data for mixtures in the system* CaO–CaO·Al_2O_3–2CaO·Fe_2O_3

Mixture No.	Composition (Weight percent)			Quenching tempera-ture	Phases present	Observed temperature of phase changes (DTA)	
	CaO	CA	C_2F			First liquid formation	Other phase changes
Mixtures having CaO·Al_2O_3 as primary phase							
				°C		°C	°C
73	16	79	5	1,428	All glass	--------	--------
				1,425	Glass+rare CA	--------	--------
				1,411	Glass+some CA	--------	--------
				1,401	Glass+CA+much $C_{12}A_7$	--------	--------
74	12	75	13	1,429	All glass	--------	--------
				1,427	Glass+a little CA	--------	--------
				1,403	Glass+CA+much $C_{12}A_7$	--------	--------
72	2	59	39	1,395	All glass	--------	--------
				1,390	Glass+very rare CA	--------	--------
				1,389	Class+some CA	--------	--------
70	3	56	41	1,361	All glass	--------	--------
				1,358	(CA liquidus)	--------	--------
				1,356	Glass+trace of CA	--------	--------
				1,352	Glass+moderate amount of CA	--------	--------
				1,331	Not sintered; CA+Fss+trace $C_{12}A_7$	--------	--------
68	9.56	65.17	25.27	1,375	(CA liquidus)	1,335	--------
				1,370	Glass+very rare CA		--------
				1,365	Glass+trace CA		
				1,357	Glass+small amount of CA		
64	7.35	62.01	30.64	1,402	All glass	1,345	--------
				1,396	(CA liquidus)		
				1,395	Glass+very rate CA		
				1,390	Glass+CA		
				1,355	Glass+much CA		
				1,350	(Fss phase appears)		
				1,348	Glass+much CA+rare Fss		

TABLE 1. *Quenching and DTA data for mixtures in the system* CaO–CaO·Al$_2$O$_3$—2CaO·Fe$_2$O$_3$—Continued

Mixture No.	Composition (Weight percent)			Quenching temperature	Phases present	Observed temperature of phase changes (DTA)	
	CaO	CA	C_2F			First liquid formation	Other phase changes
Mixtures having 12CaO·7Al$_2$O$_3$ as primary phase							
52	18.99	67.01	14	1,377	All glass	--------	--------
				1,376	($C_{12}A_7$ liquidus)	--------	--------
				1,375	Glass+rare $C_{12}A_7$	--------	--------
				1,356	Glass+moderate amount of $C_{12}A_7$	--------	--------
					Index of $C_{12}A_7=1.614\pm0.004$	--------	--------
				1,338	Glass+much $C_{12}A_7$	--------	--------
				1,335	Not sintered in packet	--------	--------
60	11.59	69.41	19.0	1,393	($C_{12}A_7$ liquidus)	1,333	--------
				1,391	Mostly glass+rare $C_{12}A_7$		
				1,389	(CA appears as second phase)		
				1,387	Glass+$C_{12}A_7$+rare CA		
				1,338	Glass+$C_{12}A_7$+CA+Fss		
54	13.19	67.81	19.0	1,351	All glass	--------	--------
				1,349	($C_{12}A_7$ liquidus)	--------	--------
				1,346	Glass+very rare $C_{12}A_7$	--------	--------
				1,336	Glass+$C_{12}A_7$+Fss	--------	--------
				1,333	Not melted	--------	--------
67	11.99	67.61	20.40	1,352	All glass	1,335	--------
				1,351	($C_{12}A_7$ liquidus)		
				1,349	Glass+rare $C_{12}A_7$		
				1,336	Glass+$C_{12}A_7$+CA+Fss		
				1,334	First liquid		
				1,333	Not sintered; $C_{12}A_7$+CA+Fss		
69	13	64	23	1,358	All glass	--------	--------
				1,357	($C_{12}A_7$ liquidus)	--------	--------
				1,356	Glass+trace $C_{12}A_7$	--------	--------
				1,342	Glass+$C_{12}A_7$+Fss+ trace CA+quench growths.	--------	--------
Mixtures having 3CaO·Al$_2$O$_3$ as primary phase							
43	24.89	70.11	5.00	1,466	Estimated C_3A liquidus	1,338	--------
				1,465	Glass+rare C_3A		
				1,460	Glass+some C_3A		
				1,381	Glass+C_3A		
				1,377	($C_{12}A_7$ appears as second phase)		
				1,375	Glass+C_3A+trace $C_{12}A_7$		
44	20.81	74.19	5.0	1,402	All glass	--------	--------
				1,400	(C_3A liquidus)	--------	--------
				1,399	Glass+small amount of C_3A	--------	--------
				1,395	Glass+C_3A	--------	--------
				1,394	($C_{12}A_7$ appears as second phase)	--------	--------
				1,392	Glass+C_3A+$C_{12}A_7$	--------	--------
45	20.59	69.41	10	1,405	All glass	--------	--------
				1,401	(C_3A liquidus)	--------	--------
				1,400	Glass+rare C_3A	--------	--------
				1,379	Glass+C_3A	--------	--------
					Index $C_3A=1.715\pm0.002$	--------	--------
				1,375	($C_{12}A_7$ appears as second phase)	--------	--------
				1,372	Glass+C_3A+very rare $C_{12}A_7$	--------	--------
9	23.57	66.43	10	1,356	Glass+C_3A	1,333	--------
				1,352	($C_{12}A_7$ appears as second phase)		
				1,348	Glass+C_3A+much $C_{12}A_7$		
13	22.26	62.74	15	1,353	Glass+lots of C_3A	1,335	--------
				1,352	Glass+C_3A+some $C_{12}A_7$		
				1,344	Glass+much C_3A+much $C_{12}A_7$		
53	18.49	62.78	18.73	1,366	All glass	--------	--------
				1,365	(C_3A liquidus)	--------	--------
				1,364	Glass+rare C_3A	--------	--------
				1,348	Glass+C_3A	--------	--------
				1,347	($C_{12}A_7$ appears as second phase)	--------	--------
				1,346	Glass+C_3A+$C_{12}A_7$+quench growths	--------	--------
46	19.37	60.63	20	1,384	All glass	--------	--------
				1,383	(C_3A liquidus)	--------	--------
				1,381	Glass+rare C_3A	--------	--------
				1,356	Glass+moderate amount C_3A	--------	--------
				1,355	(Fss appears as second phase)	--------	--------
				1,354	Glass+C_3A+a few Fss crystals	--------	--------
8	20.95	59.05	20	1,392	All glass	1,338	1,353
				1,390	(C_3A liquidus)		
				1,388	Glass+C_3A+quench growths		
				1,355	Glass+C_3A+Fss+quench growths		
61	29.77	62.23	8	1,515	All glass	--------	--------
				1,514	C_3A+glass	--------	--------
				1,512	Glass+much C_3A	--------	--------

TABLE 1. *Quenching and DTA data for mixtures in the system* $CaO–CaO \cdot Al_2O_3–2CaO \cdot Fe_2O_3$—Continued

Mixture No.	Composition (Weight percent)			Quenching temperature	Phases present	Observed temperature of phase changes (DTA)	
	CaO	CA	C_2F			First liquid formation	Other phase changes
Mixtures having $3CaO \cdot Al_2O_3$ as primary phase							
62	26.56	57.44	16	1,486	All glass	1,339	1,344
				1,483	(C_3A liquidus)		
				1,481	Glass+a few C_3A crystals		
				1,375	Glass+much C_3A		
				1,373	(Fss appears as second phase)		
				1,371	Glass+C_3A+very rare Fss		
14	19.65	55.35	25	1,384	All glass	--------	--------
				1,382	(C_3A liquidus)	--------	--------
				1,380	Trace C_3A+glass	--------	--------
				1,366	Fss+C_3A+glass	--------	--------
57	18.36	56.64	25	1,384	All glass	--------	--------
				1,382	(C_3A liquidus)	--------	--------
				1,380	Glass+rare C_3A	--------	--------
				1,372	Glass+rare C_3A	--------	--------
				1,371	(Fss appears as second phase)	--------	--------
				1,370	Glass+rare C_3A+Fss	--------	--------
63	23.74	50.26	26.0	1,444	All glass	--------	--------
				1,442	(C_3A liquidus)	--------	--------
				1,440	Glass+trace of C_3A	--------	--------
				1,387	Glass+much C_3A	--------	--------
				1,385	(Fss appears as second phase)	--------	--------
				1,383	Glass+much C_3A+some Fss	--------	--------
47	18.94	51.06	30	1,383	All glass	--------	--------
				1,382	(C_3A liquidus)	--------	--------
				1,378	Glass+small amount C_3A	--------	--------
				1,377	(Fss appears as second phase)	--------	--------
				1,370	Glass+C_3A+Fss+quench growths	--------	--------
24	25.10	46.90	28	1,439	All glass	1,389	--------
				1,439	(C_3A—CaO liquidus)		
				1,438	Trace CaO+trace C_3A+glass		
				1,436	C_3A+glass+few quench growths		
65	19.6	46.4	34	1,394	All glass	1,369	1,381
				1,392	(C_3A liquidus)		
				1,390	Glass+rare C_3A+quench growth		
				1,387	Glass+rare C_3A		
				1,385	(Fss appears as second phase)		
				1,384	Glass+C_3A+Fss		
66	20	44.3	35.7	1,391	All glass	1,388	--------
				1,390	(C_3A liquidus)		
				1,389	Glass+rare C_3A		
				1,387	Glass+rare C_3A		
				1,386	(Fss appears as second phase)		
				1,384	Glass+C_3A+Fss		
28	20.77	42.60	36.63	1,402	All glass	1,389	--------
				1,395	Glass+quench growths		
				1,392	(C_3A liquidus)		
				1,389	Glass+a little C_3A+Fss+quench growths.		
Mixtures having CaO as primary phase							
21	35.92	63.08	1	1,611	CaO in glass. Liquidus not determined.	--------	--------
				1,525	Glass+CaO	--------	--------
				1,522	(C_3A appears as second phase)	--------	--------
				1,520	Glass+CaO+rare C_3A	--------	--------
22	31.77	58.23	10	1,618	All glass	--------	--------
				1,615	(CaO liquidus)	--------	--------
				1,611	Glass+rare CaO	--------	--------
				1,500	Glass+CaO	--------	--------
				1,497	(C_3A appears as second phase)	--------	--------
				1,494	Glass+CaO+small amount of C_3A	--------	--------
23	27.44	52.56	20	1,520	All glass	1,383	--------
				1,517	(CaO liquidus)		
				1,515	Glass+rare CaO		
				1,472	Glass+CaO		
				1,470	(C_3A appears as second phase)		
				1,468	Glass+CaO+trace C_3A		
29	25.62	39.99	34.39	1,532	CaO+glass	--------	--------
25	21.57	40.43	38.00	1,398	All glass	1,388	--------
				1,397	(CaO liquidus)		
				1,396	Trace CaO+glass		
				1,395	CaO+C_3A+glass		

TABLE 1. *Quenching and DTA data for mixtures in the system* $CaO–CaO \cdot Al_2O_3–2CaO \cdot Fe_2O_3$—Continued

Mixture No.	Composition (Weight percent)			Quenching temperature	Phases present	Observed temperature of phase changes (DTA)	
	CaO	CA	C_2F			First liquid formation	Other phase changes
Mixtures having CaO as primary phase							
G64 [a]	21.20	38.80	40.00	1,380	Barely sintered, X-ray shows Fss + C_3A.	--------	--------
				1,384	do	--------	--------
				1,388	Little glass+much Fss+rare CaO +C_3A+growths.	--------	--------
				1,390	Little glass+Fss+little CaO+C_3A +growths.	--------	--------
				1,394	Mostly glass+rare CaO+little Fss +growths.	--------	--------
				1,400	Mostly glass+rare CaO, no Fss seen	--------	--------
48	23.18	28.32	48.50	1,473	All glass	1,387	1,399
				1,470	(CaO liquidus)		
				1,468	Glass+a little CaO		
32	21.13	28.99	49.88	1,455	All glass	1,389	1,402
				1,453	(CaO liquidus)		
				1,451	Glass+a little CaO		
49	19.59	18.11	62.3	1,530	Glass+trace of CaO+quench growths	1,415	--------
				1,498	Glass+trace of CaO		
				1,480	Glass+small amount of CaO		
35	16.73	18.74	64.53	1,542	Glass+quench growth	1,416	--------
				1,536	(CaO liquidus)		
				1,532	Glass+trace of CaO+quench growths		
50	12.63	10.37	77	1,539	Glass+very rare CaO+quench growths.	1,425	--------
				1,534	Glass+rare CaO+quench growths		
				1,520	Glass+CaO+quench growths		
51	4	-------	96	1,449	Glass+quench growths	1,438	--------
				1,440	Glass+CaO+quench growths		
Mixtures having Fss as primary phase							
58	17.77	62.23	20	1,370	All glass	--------	--------
				1,355	(Fss liquidus)	--------	--------
				1,351	Glass+rare Fss	--------	--------
				1,341	Glass+Fss	--------	--------
				1,340	($C_{12}A_7$ appears as second phase)	--------	--------
				1,339	Glass+Fss+trace of $C_{12}A_7$	--------	--------
78	12.46	62.01	25.53	1,359	All glass	--------	--------
				1,356	(Fss liquidus)	--------	--------
				1,352	Glass+Fss	--------	--------
71	8.0	58	34	1,379	All glass	--------	--------
				1,374	(Fss liquidus)	--------	--------
				1,370	Glass+a little Fss	--------	--------
7	18.34	51.66	30	1,384	All glass	1,334	1,367
				1,383	(Fss liquidus)		
				1,381	Glass+trace of Fss		
				1,377	Glass+moderate amount Fss		
75	16.2	50.0	33.8	1,400	All glass	--------	--------
				1,397	(Fss liquidus)	--------	--------
				1,395	Glass+small amount of Fss	--------	--------
				1,393	Glass+Fss	--------	--------
15	17.03	47.97	35	1,390	All glass	1,338	1,366
				1,389	(Fss liquidus)		
				1,386	Glass+Fss		
				1,370	Glass+Fss+C_3A		
76	15.8	48.3	35.9	1,411	All glass	--------	--------
				1,374	Glass+much Fss	--------	--------
36	18.45	43.84	37.71	--------	--------	1,385	--------
39	17.24	44.49	38.27	1,400	All glass	1,385	--------
				1,396	(Fss liquidus)		
				1,393	Glass+Fss+quench growths		
				1,391	(C_3A appears as second phase)		
				1,389	Glass+Fss+C_3A+quench growths		
C_6A_2F	16.02	45.15	38.83	1,398	All glass	1,367	1,389
				1,397	(Fss liquidus)		
				1,396	Glass+a little Fss		
				1,388	Glass+much Fss		
40	13.50	46.50	40	--------	--------	1,332	1,356
27	11.06	47.81	41.13	1,381	Glass+Fss+quench growths	1,342	1,382

[a] Made by M. A. Swayze.

TABLE 1. *Quenching and DTA data for mixtures in the system* CaO–CaO·Al$_2$O$_3$–2CaO·Fe$_2$O$_3$—Continued

Mixture No.	Composition (Weight percent)			Quenching temperature	Phases present	Observed temperature of phase changes (DTA)	
	CaO	CA	C^2F			First liquid formation	Other phase changes
Mixtures having Fss as primary phase							
6	15.72	44.28	40	1,403 1,397	All glass Glass+quench growths	1,371	1,386
26	21.18	38.82	40	1,394 1,393 1,386	All glass Glass+Fss+CaO+quench growths No glass, Fss+C_3A+quench growths	1,388	-------
16	14.41	40.59	45	1,410	All glass	1,383	-------
5	13.10	36.90	50	1,420 1,418 1,416	All glass (Fss liquidus) Glass+Fss	1,399	-------
31	16.20	30.79	53.01	1,411 1,408 1,406 1,405	All glass Glass+quench growth (Fss liquids) Glass+rare Fss	1,390	1,401
37	14	31.61	54.39	----------	----------	1,388	1,399
C_4AF	11.54	32.52	55.94	1,426 1,424 1,422	All glass (Fss liquidus) Glass+trace of Fss	1,403	----------
55	8.82	33.51	57.67	1,410 1,409 1,408 1,400	All glass (Fss liquidus) Glass+Fss+quench growths Glass+Fss+quench growths	1,338	1,399
30	6.35	34.41	59.24	1,410 1,361	Glass+quench growths Glass+some Fss+quench growths	1,323	1,366
4	10.48	29.52	60	1,434 1,421	Glass+quench growths Glass+Fss+quench growths	---------- ----------	---------- ----------
17	9.17	25.83	65	1,423 1,421 1,419	Glass+few quench growths (Fss liquidus) Glass+Fss+quench growths	1,412	1,422
3	7.86	22.14	70	----------	----------	1,428	1,433
34	11.73	19.87	68.40	1,425 1,416 1,414 1,412	Glass+quench growths Glass+Fss+quench growths (CaO appears as second phase) Glass+Fss+CaO+quench growths	1,416	----------
38	9.89	20.28	69.83	1,418 1,417 1,416	Glass+Fss+quench growths CaO appears as second phase Glass+Fss+a little CaO+quench-growths.	1,415	1,423
41	8.65	20.57	70.78	----------	----------	1,418	-------
C_6AF_2	7.40	20.85	71.75	----------	----------	1,427	-------
42	4.57	21.48	73.95	----------	----------	1,420	-------
33	1.74	22.12	76.14	----------	----------	1,206	1,409
18	6.55	18.45	75	----------	----------	1,421	1,428
59	6.04	15.96	78	1,421 1,400 1,391	Glass+Fss+quench growths Glass+Fss+quench growths Glass+Fss+small CaO crystals	1,423	-------
77	7.0	11	82	1,430 1,422 1,421 1,420	Glass+very rare CaO Glass+Fss+quench growths (CaO appears as second phase) Glass+Fss+CaO+quench growths	------- ------- ------- -------	------- ------- ------- -------
19	3.92	11.07	85	-------	----------	1,426	1,430
1	2.62	7.38	90	1,464 1,457	Glass+quench growths Glass+quench growths	------- -------	------- -------
20	1.31	3.69	95	-------	----------	1,430	-------
C_2F	-------	-------	100	-------	----------	1,439	-------

Temperatures reported are accurate within ±5° C. Experience with repeated determinations of temperature for the same phase change indicates that the temperatures are reproducible within ±2° C. In order to conserve space, not all of the data are presented here but only those that suffice to establish the phase relations. The compositions of mixtures studied are shown in figure 2.

Primary phase regions occur for CaO, 3CaO·Al$_2$O$_3$, 12CaO·7Al$_2$O$_3$, CaO·Al$_2$O$_3$, and calcium aluminoferrite solid solutions (Fss). The three calcium aluminates contain small amounts of CaO and Fe$_2$O$_3$ in

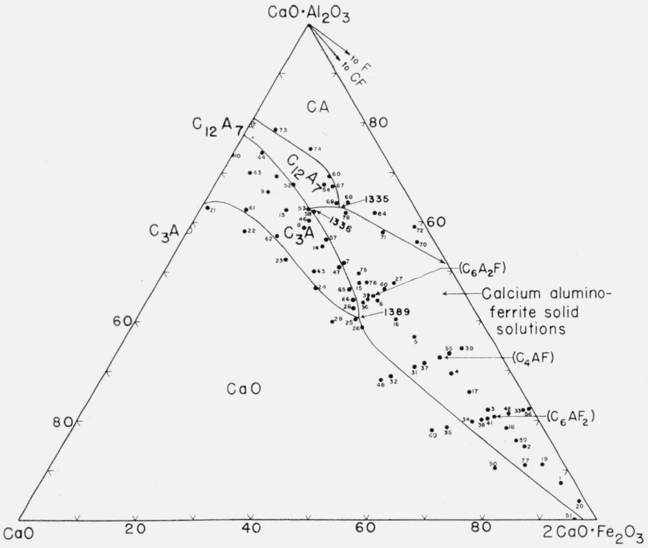

FIGURE 2. *Equilibrium diagram of the pseudo-ternary system* CaO-CaO·Al$_2$O$_3$-2CaO·Fe$_2$O$_3$ *showing compositions studied and primary phases.*

solid solution. The approximate limits of the calcium aluminate solid solutions, shown in figure 1, are taken from data reported by McMurdie [6] and by Yamauchi [7].

In general, phase boundaries and two of the invariant points determined are close to those reported by Swayze [8]. Some minor differences (table 2) exist in the compositions and temperatures of the invariant points at which (1) CaO, 3CaO·Al$_2$O$_3$, and a calcium aluminoferrite solid solution (Fss) and (2) 3CaO·Al$_2$O$_3$, 12CaO·7Al$_2$O$_3$, and Fss may occur in equilibrium with a liquid phase. To recheck differences between previously published data and the present work, a direct comparison has been made between mixture G64 synthesized by Swayze as the eutectic composition, and our No. 26 which has almost the same composition. The results are listed in table 1. In our study of Mix G64, all samples were held at temperature for 2 hr as described in the section headed Experimental Methods.

The composition determined in the present work for a third invariant point (E$_3$, fig. 1) at which 12CaO·7Al$_2$O$_3$, CaO·Al$_2$O$_3$, and Fss can coexist with liquid is in reasonable agreement with that of McMurdie [6], although the temperature is approximately 10° higher than that reported by him.

The diagram presented in Swayze's report depicts a primary phase region for 6CaO·2Al$_2$O$_3$·Fe$_2$O$_3$ distinct from the region of variable Fss composition. In the present work, however, the composition of the calcium aluminoferrite phase in equilibrium with liquid was found by X-ray powder diffraction measurements to change continuously with temperature over its primary phase region, and no second iron-bearing phase appeared. Along the E$_2$-E$_3$ boundary (fig. 1), however, the change in the Fss composition was so slight that it was not considered in constructing the diagram.

The compositions of the Fss phases in equilibrium at the invariant points and the assemblages of final crystallization products also differ from those reported by previous investigators [2, 6, 8]. These results will be discussed in greater detail in the sections that follow.

3.2. Calcium Aluminoferrite Solid Solutions

In figures 1[5] and 3, a single-phase region of calcium aluminoferrite solid solutions is designated by the shaded area extending from 2CaO·Fe$_2$O$_3$ toward the CaO-CaO·Al$_2$O$_3$ boundary of the system.

X-ray powder diffraction patterns of devitrified glasses with compositions along the line X–Y (fig. 3) confirmed 3CaO·Al$_2$O$_3$ and Fss to be the final products of crystallization for 6CaO·2Al$_2$O$_3$·Fe$_2$O$_3$ and neighboring glasses with higher CaO contents. These compositions are, therefore, not in the single-phase (solid solution) region, but are on the high-CaO side of it. Mixtures No. 40 and 27, on the other hand, each showed CaO·Al$_2$O$_3$ and Fss as devitrification products and are on the low-CaO side of the Fss band.

In figure 4 the ratios of intensities of selected diffraction peaks for 3CaO·Al$_2$O$_3$ or CaO·Al$_2$O$_3$ to those of a peak of the tungsten internal standard in the same pattern have been plotted against the

---

[5] For reasons of limited space, compounds and phases are referred to by symbols. For example: C=CaO; A=Al$_2$O$_3$; F=Fe$_2$O$_3$; and Fss=calcium-aluminoferrite solid solution. Thus, C$_4$AF=4CaO·Al$_2$O$_3$·Fe$_2$O$_3$.

TABLE 2. *Invariant points for the pseudoternary system* CaO–CaO·Al$_2$O$_3$–2CaO·Fe$_2$O$_3$n

Phases	Authority	Composition percentage						Temperature, ±5° C
		CaO	Al$_2$O$_3$	Fe$_2$O$_3$	CaO	CaO·Al$_2$O$_3$	2CaO·Fe$_2$O$_3$	
								°*C*
CaO–C$_3$A–Fss (or C$_4$AF)	W. C. Hansen, L. T. Brownmiller, and R. H. Bogue.	54	37	9	--------	--------	--------	1,340
	H. F. McMurdie	53	32	15	--------	--------	--------	1,370
	M. A. Swayze	51.4	25.0	23.6	--------	--------	--------	1,380
	Present investigation	51.1	26.5	22.4	20.8	41.0	38.2	1,389
C$_3$A–C$_{12}$A$_7$ (or C$_5$A$_5$)–Fss (also C$_4$AF or C$_6$A$_2$F).	W. C. Hansen, L. T. Brownmiller, and R. H. Bogue.	47	43	10	--------	--------	--------	1,335
	H. F. McMurdie	48	38	14	--------	--------	--------	1,335
	M. A. Swayze	48.5	40.5	11.0	--------	--------	--------	1,335
	Present investigation	48.4	40.3	11.3	18.3	62.4	19.3	1,336
C$_{12}$A$_7$ (or C$_5$A$_3$)–CA–Fss (or C$_4$AF).	W. C. Hansen, L. T. Brownmiller, and R. H. Bogue.	42	40	18	--------	--------	--------	1,320
	H. F. McMurdie	45	40	15	--------	--------	--------	1,315
	Present investigation	45.1	40.6	14.2	12.8	63.0	24.2	1,335

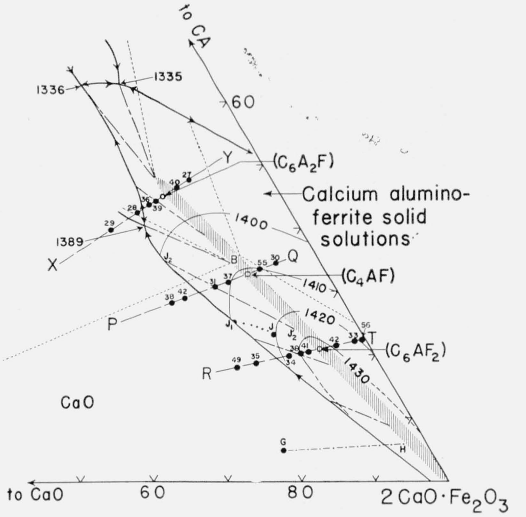

FIGURE 3. *Calcium aluminoferrite solid-solution regions in the pseudo-ternary system* CaO-CaO·Al$_2$O$_3$-2CaO·Fe$_2$O$_3$ *with tie lines and typical crystallization paths.*

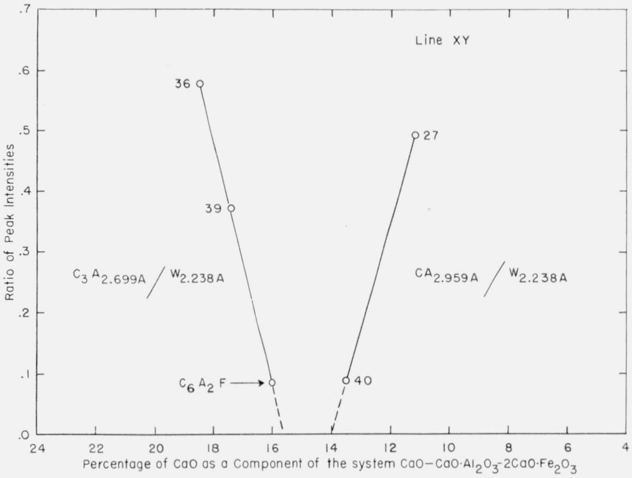

FIGURE 4. *Relationship between the CaO content and the relative intensities of selected* 3CaO·Al$_2$O$_3$ *and* CaO·Al$_2$O$_3$ *peaks as compared with standard tungsten peaks in X-ray powder diffraction patterns of devitrified glasses with compositions along the line XY (see fig. 3).*

percentage of the CaO component for these devitrified glasses. The approximate width (2% CaO) of the solid-solution band in this region has been determined by extrapolating the two curves obtained by the above procedure to a zero ratio. A similar treatment (fig. 5) gives the approximate width of the Fss band along line P–Q (fig. 3) at 4CaO·Al$_2$O$_3$·Fe$_2$O$_3$.

For compositions on the line R–T in figure 3, the secondary phase on the low CaO side of 6CaO·Al$_2$O$_3$·2Fe$_2$O$_3$ is CaO·Fe$_2$O$_3$ (with a small amount of CaO·Al$_2$O$_3$ in solid solution). Most of the principal diffraction maxima for the latter compound correspond closely to those for some members of the calcium-aluminoferrite solid-solution series. Because of this interference the low CaO limit of the Fss band could not be determined as closely in this region by the X-ray diffraction method. It was observed (table 1), however, that the differential temperature curves in DTA patterns of mixtures with compositions found by the X-ray method to be near but outside of the solid-solution band contained two peaks, whereas curves of mixtures within the band contained only one. This characteristic made it possible to define more closely than by the X-ray method the limit of solid solution in the 6CaO·Al$_2$O$_3$·2Fe$_2$O$_3$ region in the direction away from the CaO vertex.

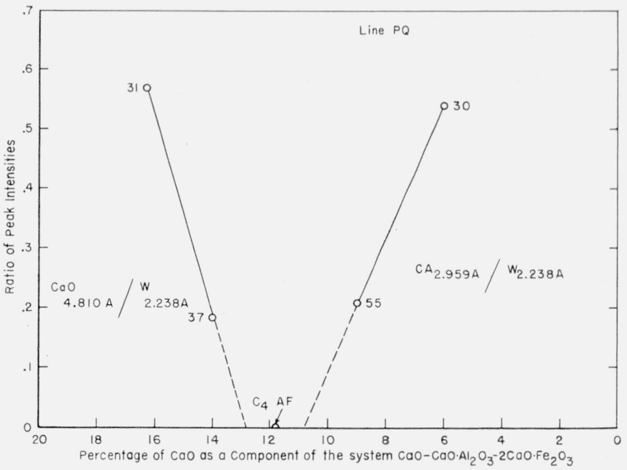

FIGURE 5. *Relationship between the CaO content and the relative intensities of selected* CaO *and* CaO·Al$_2$O$_3$ *peaks as compared with standard tungsten peaks in X-ray powder diffraction patterns of devitrified glasses with compositions along the line PQ (see fig. 3).*

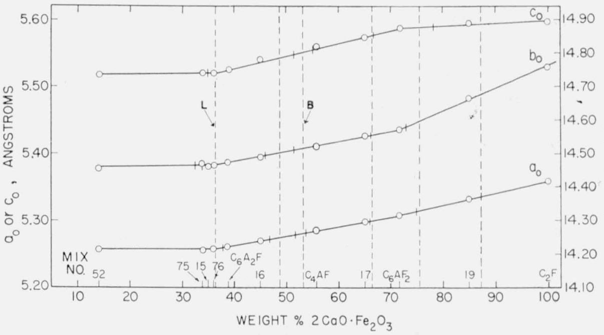

FIGURE 6. *Selected interplanar spacings* (d_{hkl}) *characteristic of the iron-bearing solid-solution phase for mixtures along the line* C_2F-*L (fig. 1).*

Dotted lines show compositions of Fss phase at ends of tie lines.

Unit-cell dimensions for the Fss phase in completely crystallized mixtures with compositions in or near the single-phase (solid-solution) band are plotted as a function of composition in figure 6. These dimensions are based on interplanar spacings obtained from X-ray powder diffraction patterns by the authors, together with indices reported by Malquori and Cirilli [10]. A change in the slopes of the curves for a$_0$, b$_0$, and c$_0$ in figure 6 occurs near the composition 6CaO·Al$_2$O$_3$·2Fe$_2$O$_3$, which may represent an ordering of the structure. Lattice parameters continue to change with further compositional changes to point L, however, and the region is, therefore, shown on the phase diagram as one of continuous solid solution.

TABLE 3. *Significant calcium aluminoferrite solid-solution compositions for the pseudoternary system* CaO-$CaO \cdot Al_2O_3$-$2CaO \cdot Fe_2O_3$

Designation	Authority	Composition percentage						Molecular formula
		CaO	Al_2O_3	Fe_2O_3	CaO	$CaO \cdot Al_2O_3$	$2CaO \cdot Fe_2O_3$	
1. Solid solution limit (high-Al_2O_3 end).	W. C. Hansen, L. T. Brownmiller, and R. H. Bogue.	46.1	21.0	32.9	11.4	32.6	56.0	$4CaO \cdot Al_2O_3 \cdot Fe_2O_3$
C_6A_2F	M. A. Swayze	48.07	29.12	22.81	16.0	45.1	38.8	$6CaO \cdot 2Al_2O_3 \cdot Fe_2O_3$
Solid solution limit	T. Yamauchi	-------	-------	-------	-------	-------	-------	$6.2CaO \cdot 2.2Al_2O_3 . Fe_2O_3$
Solid solution limit	G. L. Malquori and C. L. Cirilli.	-------	-------	20.5	-------	-------	34.9 by weight	
Solid solution limit Point L (fig. 1).	Present investigation	47.78	31.13	21.09	15.7	48.0	36.3	$6.37CaO \cdot 2.28Al_2O_3 . Fe_2O_3$
2. Composition at CaO-C_3A-Fss invariant point:								
Point B (fig. 1)	Present investigation	45.95	23.06	30.99	11.50	35.75	52.75	$4.3CaO \cdot 1.1Al_2O_3 \cdot Fe_2O_3$
Point VIII	M. A. Swayze	45.57	18.01	36.42	10.07	27.92	62.00	
C_4AF	W. C. Hansen, L. T. Brownmiller, and R. H. Bogue.	46.1	21.0	32.9	11.4	32.6	56.0	$4CaO \cdot Al_2O_3 \cdot Fe_2O_3$

In figures 1 and 7, point L designates the limit of solid solution, determined in the present investigation, in the direction of the CaO-$CaO \cdot Al_2O_3$ boundary. The composition represented by point L agrees well with those reported by Yamauchi [7] and by Malquori and Cirilli (see table 3). It contains less ferric oxide than the composition $6CaO \cdot 2Al_2O_3 \cdot Fe_2O_3$. Composition L is the solid solution in equilibrium at invariant points E_2 and E_3. The solid solution in equilibrium at point E_1 corresponds to point B (table 3).

The changing composition of the calcium-aluminoferrite solid-solution crystals (Fss) in equilibrium with liquid with changing temperature is depicted on the phase diagram (figs. 1 and 3) by a series of tie lines.

Throughout the Fss primary region, large variations in composition have little effect on liquidus temperatures. This behavior causes the composition of the liquid formed in a mixture in this region to reach a primary-phase boundary only a few degrees below the liquidus temperature. The tie lines of importance, therefore, are those that indicate the compositions of the Fss phase in equilibriun with liquids on the phase boundaries and at invariant points that bound the Fss region. Seven such tie lines have been established in this investigation.

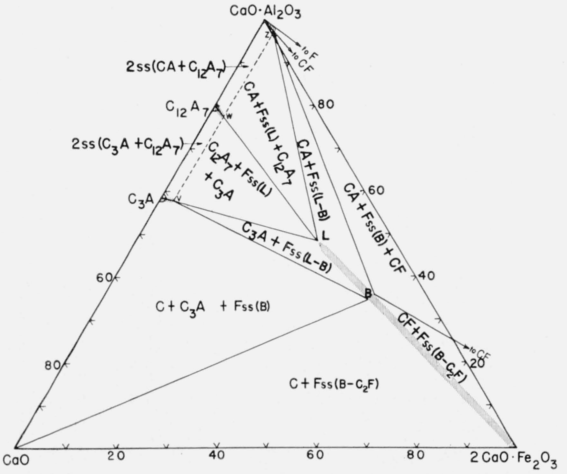

FIGURE 7. *Final products of crystallization in pseudo-ternary system* CaO-$CaO \cdot Al_2O_3$-$2CaO \cdot Fe_2O_3$.

3.3. Crystallization in the System

In the pseudoternary system CaO-$CaO \cdot Al_2O_3$-$2CaO \cdot Fe_2O_3$ there are 11 areas in which compositions may fall with regard to their final products of equilibrium crystallization. These are designated in figure 7. In only 4 of these regions is crystallization completed (or melting begun) at an invariant point. These are the composition triangles [6] with their respective invariant temperatures:

(1) CaO-$3CaO \cdot Al_2O_3$-Fss(B)	1,389° C.
(2) $3CaO \cdot Al_2O_3$-$12CaO \cdot 7Al_2O_3$-Fss(L)	1,336° C.
(3) $12CaO \cdot 7Al_2O_3$-$CaO \cdot Al_2O_3$-Fss(L)	1,335° C.
(4) $CaO \cdot Al_2O_3$-Fss(B)-$CaO \cdot Fe_2O_3$	(Invariant point outside pseudosystem limits.)

Mixtures with compositions in any one of the above four triangles will, on heating under equilibrium conditions, begin to melt at the temperature indicated. The composition of the first liquid formed will be that of the invariant point (table 2 and fig. 1) at which the three designated crystalline phases can exist in equilibrium with liquid. Conversely, on cooling these mixtures, the last bit of liquid will have the composition of the invariant point and will disappear at the invariant temperature. The specimen will then consist of the three crystalline phases at the vertices of the triangle.

Compositions in 6 of the areas complete their crystallization on a phase boundary. These two-phase areas are designated in figure 7 by their final products of equilibrium crystallization, viz:

(1) $CaO \cdot Al_2O_3 +$ Fss(L-B)
(2) $3CaO \cdot Al_2O_3 +$ Fss(L-B)
(3) $CaO +$ Fss(B-C_2F)
(4) $CaO \cdot Fe_2O_3 +$ Fss(B-C_2F)
(5) 2 solid solutions ($3CaO \cdot Al_2O_3 + 12CaO \cdot 7Al_2O_3$)
(6) 2 solid solutions ($12CaO \cdot 7Al_2O_3 + CaO \cdot Al_2O_3$).

---

[6] As indicated in figures 1 and 7, all of the compounds listed, except CaO, contain some material in solid solution. The variations in composition are small, however, and of little importance in comparison with the range of calcium aluminoferrite solid solutions (Fss). For convenience the symbol "ss", indicating a solid solution, is used in the text only to designate the calcium aluminoferrite series, or single compositions in this series.

In each of the six areas, the temperature at which a liquid is first formed on heating, or disappears on cooling, varies with composition. At least one of the products of crystallization, however, will consist of a solid solution whose composition will also vary with the composition of the mixture.

Thus for the triangle labeled "C+Fss(B-C_2F)" (fig. 7), the products at complete equilibrium crystallization will consist of CaO and a calcium aluminoferrite solid solution whose composition is between point B and C_2F.

For a given mixture in one of the six 2-phase areas, the final composition of the Fss phase is determined by a line from the composition of the other crystallization product through the composition of the mixture, and extended to the boundary of the *single-phase* Fss area (largest shaded area). The point at which the line intersects this boundary is the composition of the Fss crystallization product. An example in figure 3 is composition G; a line from the CaO vertex through G intersects the boundary of the shaded area at H, the composition of the Fss phase in mixture G when crystallization is completed.

In the 11th area, the shaded Fss area, all compositions after crystallization consist of one phase, a calcium aluminoferrite solid solution having the same composition as the original mixture.

In addition to the 11 areas discussed above, shading near $3CaO\cdot Al_2O_3$ and $12CaO\cdot 7Al_2O_3$ in figures 1, 7, and 8 indicates solid solutions along the lines $3CaO\cdot Al_2O_3$-V and $12CaO\cdot 7Al_2O_3$-W respectively. There is also a small shaded area near $CaO\cdot Al_2O_3$ representing a ternary solid solution just beyond the pseudosystem boundary. The product of crystallization of compositions in each of these regions is also a single solid solution.

Compositions in the shaded portions of the diagram complete their crystallization at temperatures for corresponding points on the solid-solution solidus. These points are below the projected liquidus surface in figure 1, and for those regions the solidus temperatures cannot be determined from the figure. All mixtures studied do have Fss as an equilibrium product of crystallization and the first liquid formation temperature is the solidus temperature for the Fss phase that is present. The temperatures of first liquid formation are given for most of the mixtures in table 1, and for mixtures in the Fss primary phase region these solidus temperatures can be compared directly with the corresponding Fss liquidus temperatures.

The pseudosystem CaO-$CaO\cdot Al_2O_3$-$2CaO\cdot Fe_2O_3$ is unusual inasmuch as it contains examples of most of the major types of equilibrium crystallization. Furthermore, the system contains an extensive series of ternary solid solutions with intermediate and end members (B and L, respectively, fig. 1) that exhibit some of the characteristics of incongruently melting compounds. These complicate the crystallization process.

It should be noted in figures 1, 3, and 8 that the liquidus maximum on the phase boundary separating the $3CaO\cdot Al_2O_3$, and the Fss primary phase regions occurs not at the intersection of the boundary with the line V-B, but at a nearby point where the tie lines from V and from the single-phase Fss region (the large, shaded area) become collinear. Similarly, the maximum on the boundary between $CaO\cdot Al_2O_3$ and Fss regions occurs at the point where the tie lines to Z and the single-phase Fss region become collinear. A similar configuration was reported by Roy and Osborn [14] for the system $Li_2O\cdot SiO_2$-$Li_2O\cdot Al_2O_3\cdot 4SiO_2$-$SiO_2$.

Almost any composition to be encountered in the ternary system can be classified under one of four types of crystallization to be discussed here. The exceptions are compositions in the shaded regions (figs. 1 and 7) for which, as mentioned previously, only approximate liquidus temperatures and final crystallization products can be determined from the ternary diagrams.

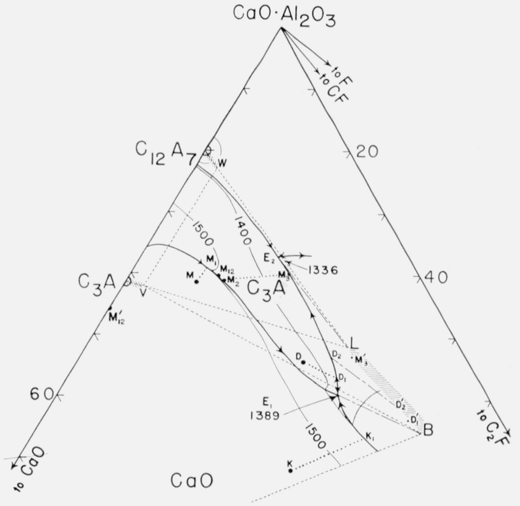

FIGURE 8. *A portion of the equilibrium diagram showing paths of crystallization followed by typical mixtures within the system.*

C_3A and $C_{12}A_7$ solid solutions are treated as having the constant composition V and W.

For convenience, the equilibrium crystallization of compositions in the system will be discussed in terms of cooling chosen mixtures from a temperature at which they are completely melted to a temperature at which all liquid disappears. It will be assumed that equilibrium exists in all phases throughout the process, although this situation may be difficult to approximate in actual practice.

As the first example, consider the composition (fig. 8) represented by point K in the triangle CaO-C_3A-B. On cooling this mixture, crystals of CaO appear at the liquidus temperature. With continued cooling, CaO continues to crystallize and the composition of the liquid moves along the line K-K_1 until it reaches the point K_1 on the CaO-Fss phase boundary. With further cooling, the composition of the liquid follows the CaO-Fss phase boundary from K_1 to the eutectic at E_1. Both Fss and CaO are in equilibrium with liquid in this temperature range. After the liquid composition has reached E_1 (at the eutectic temperature, 1,389° C), crystals of $3CaO \cdot Al_2O_3$ appear. At the minimum heat content, the charge will be completely crystallized and will consist only of CaO, Fss(B), and $3CaO \cdot Al_2O_3$.

The crystallization of a composition M (Mix No. 22, table 1) in the triangle V-W-L follows a somewhat more complex pattern. On cooling M from its liquidus temperature of 1,615° C, CaO crystallizes as the primary phase and the liquid composition moves directly away from the CaO vertex along a line M-M_1. At M_1, $3CaO \cdot Al_2O_3$ appears as a secondary crystalline phase. With further cooling, the liquid composition then moves down the boundary between the CaO and $3CaO \cdot Al_2O_3$ regions until it reaches point M_2. In the temperature range in which the liquid composition is changing from M_1 to M_2, the mean composition of the solid phases is changing from CaO to $3CaO \cdot Al_2O_3$. Neglecting the small amount of solid solution in the calcium aluminate, the mean composition of the solids at any temperature in this range is obtained by drawing a line from the corresponding liquid composition M_{12} through M (the composition of the mixture) to the point M'_{12} at which it intersects the system boundary CaO-$3CaO \cdot Al_2O_3$. When the composition of the liquid reaches M_2, all of the crystalline CaO will have dissolved and the composition of the solid phase present will be $3CaO \cdot Al_2O_3$. On further cooling, therefore, the composition of the liquid will move directly across the $3CaO \cdot Al_2O_3$ primary phase region along the line M-M_2-M_3. At M_3 crystals of a calcium aluminoferrite solid solution having the composition indicated by point M'_3 at the end of the interpolated tie line, M_3-M'_3, will then begin to crystallize. As the temperature is lowered, the composition of the liquid will move along the $3CaO \cdot Al_2O_3$-Fss phase boundary to E_2 at 1,336° C at which point crystallization will be completed. Mixture M will then be composed of crystals of $3CaO \cdot Al_2O_3$, $12CaO \cdot 7Al_2O_3$, and Fss (L).

During crystallization, the changing liquid compositions for mixtures in the Fss primary phase region may be represented on the phase diagram by curved lines. The curvature results from the fact that in this region the composition of the solid (Fss) phase is also changing with temperature.

In figure 3, a portion of the approximate crystallization path for mixture J in the Fss primary-phase region and the composition triangle CaO-B-C_2F is designated by the dotted line J-J_1. This path is typical of those for other mixtures in the same region. Additional crystallization paths in the same area are not shown inasmuch as compositions in this area form liquids having compositions on the CaO-Fss phase boundaries at only a few degrees below the respective liquidus temperatures of the mixtures.

The composition J_1 is defined by that member of the indicated family of the tie lines which passes through J. After reaching J_1, the composition of the liquid on further cooling will follow the CaO-Fss phase boundary in the direction of decreasing temperature until the solid solution, as defined by the family of tie lines, reaches a composition J'_2 on the straight line defined by J and the CaO vertex. The liquid composition at the conclusion of crystallization is the end of the tie line from J'_2, or the point J_2. The final products of equilibrium crystallization for mixture J will thus be CaO and an Fss phase having the composition J'_2.

Other tie lines in the phase diagram designate compositions of the Fss phase found to coexist with designated liquid compositions along the phase boundaries. For intermediate points (such as D_1, fig. 8), the approximate compositions of the coexisting liquid and solid phases can be determined by graphical interpolation of the given tie lines. For each mixture in a two-phase area, the point which represents the composition of the liquid when crystallization is completed will be on the phase boundary at the end of the tie line that connects with the composition of the final Fss crystallization product for the mixture.

Mixture D (fig. 8) represents another typical composition in a two-phase area. Here $3CaO \cdot Al_2O_3$ is the primary phase and it continues to crystallize as the temperature is lowered until the liquid reaches the phase boundary at D_1. At this point, an infinitesimal amount of Fss having approximately the composition D'_1 (on an interpolated tie line, D_1-D'_1) begins to crystallize. The liquid composition then moves along the C_3A-Fss boundary until the solid solution composition reaches a point D'_2 defined by the straight line through V and D. At the completion of crystallization, the liquid composition is D_2, the end of the tie line from D'_2. Mixture D is then composed of $3CaO \cdot Al_2O_3$, and Fss of composition D'_2.

4. Application to Portland Cement Chemistry

The extent to which information on the ternary system can be applied directly to the manufacture of portland cement clinker containing many components is, of course, limited. Nevertheless, because of similarity of the phases actually observed in commercial clinkers to some of those appearing in simpler systems, useful extrapolations of phase relations in these systems can help to explain the behavior of the more complex compositions.

It is generally conceded, as a result of previous investigations [2, 7, 8, 9], that the principal iron-bearing phase in portland cement clinker is essentially a calcium aluminoferrite of variable composition. In commercial clinkers it is likely that this phase contains also small amounts of additional components in solid solution. As a first approximation, however, its composition can be considered as falling within the limits of the shaded single-phase Fss area on the phase diagram in figure 1.

It is evident from figures 1 and 7 that even the composition of the final Fss phase, formed by complete equilibrium crystallization, can vary widely with different mixtures in the system. This variability results from the fact that there are wide ranges of composition (the six 2-phase areas) for which crystallization is completed on a phase boundary, rather than at an invariant point. The variability applies to the temperature at which liquid is first formed or disappears in the different mixtures as well as to the composition of the Fss phase.

Only in the single-phase Fss region and the two-phase CaO-Fss region will the Al_2O_3/Fe_2O_3 ratio of the Fss phase always be the same as that of the original mixture.

The one- and two-phase areas in the ternary system (fig. 7) may be expected to bound analogous regions in multicomponent clinker systems in which both the final composition of the Fss phase and the solidus temperature will vary with the composition of the mixture. *Even if equilibrium were attained,* therefore, for commercial portland clinkers the temperature at which liquid is first formed during burning, the quantity of liquid produced in the hot zone of the kiln, and the constitution of the clinker can differ considerably for cement raw mixtures of different Al_2O_3/Fe_2O_3 ratios. The Al_2O_3/Fe_2O_3 weight ratio in the iron-bearing phase can presumably vary with different mixtures from 0 to 1.476, with accompanying effects on the percentages of the other clinker constituents.

Although the presence of Fe_2O_3 in the mix causes the formation of a liquid phase at a lower temperature than if it were absent, increasing the percentage of Fe_2O_3 in the raw mix does not necessarily cause easier burning, but may even have the opposite effect. Study of figure 1 reveals that mixtures whose crystallization is completed along the CaO-Fss phase boundary, or at E_1 (eutectic temperature, 1,389° C) will be more difficult to burn than mixtures completing their crystallization at invariant points E_2 and E_3.

Optimum conditions for proportioning and burning given raw materials of known chemical compositions to produce clinker of the desired constitution and burning characteristics cannot be determined from the phase diagram for the ternary system alone. Additional work is still required on portions of the quaternary system CaO-Al_2O_3-Fe_2O_3-SiO_2. Specifically needed in the four-component system are additional tie lines showing the compositions of the Fss phase in equilibrium with liquids along phase boundaries, and a further subdivision of the system into composition spaces that define the final products of crystallization within each region. Such a subdivision provides information on the quaternary system analogous to that given in figure 7 for the ternary system.

The authors are indebted to M. A. Swayze for his generous cooperation in making available to them for reference, his slides, mixtures, and notes on the ternary system CaO-5CaO·$3Al_2O_3$-2CaO·Fe_2O_3. They also express thanks to A. C. Bonanno and R. L. Wadlinger for their help in obtaining X-ray and quenching data presented in this paper.

5. References

[1] H. LeChatelier, Experimental researches on the constitution of cements and the theory of their setting, Compt. rend. **94**, 867 (1882).

[2] W. C. Hansen, L. T. Brownmiller, and R. H. Bogue, Studies on the system calcium oxide-alumina-ferric oxide, J. Am. Chem. Soc. **50**, 396 (1928); PCAF Paper 13.

[3] F. M. Lea, T. W. Parker, Investigations on a portion of the quaternary system CaO-Al_2O_3-SiO_2-Fe_2O_3: The quaternary system CaO-2CaO·SiO_2-5CaO·$3Al_2O_3$-4CaO·Al_2O_3·Fe_2O_3, Phil. Trans. Royal Soc. [A] **234** (731) 1 (1934).

[4] W. Büssem, and A. Eitel, The structure of pentacalcium trialuminate, Z. Krist. **95**, 175 (1936); W. Büssem, X-rays and cement chemistry, proc. symposium on chemistry of cements, Stockholm, p. 141 (1938).

[5] T. Thorvaldson and W. G. Schneider, the composition of the "5:3" calcium aluminate, Can. J. Research [B] **19**, 109 (1941).

[6] H. F. McMurdie, Studies on a portion of the system CaO-Al_2O_3-Fe_2O_3, J. Research NBS **18**, 475 (1937) RP 987.

[7] T. Yamauchi, A study on the celite part: I. The system CaO-Fe_2O_3, J. Japan Ceram. Assoc. **45**, 279; II. On the brownmillerite, p. 361–75; III. The system 3CaO·Al_2O_3-2CaO·Fe_2O_3, p. 433–46; IV. The system 5CaO·$3Al_2O_3$-2CaO·Fe_2O_3. p. 614–31; V. The system 3CaO·Al_2O_3-5CaO·$3Al_2O_3$-2CaO·Fe_2O_3, p. 880–96 (1937); VII. The systems CaO-Al_2O_3-Fe_2O_3 and CaO-Al_2O_3-Fe_2O_3-SiO_2, J. Japan Ceram. Assoc. **46**, 66 (1938).

[8] M. A. Swayze, A report on studies of (1) the ternary system CaO-C_5A_3-C_2F, (2) the quaternary system CaO-C_5A_3-C_2F-C_2S, and (3) the quaternary system as modified by 5% magnesia, part I, Am. J. Sci. **244**, 1 (1946).

[9] M. A. Swayze, A report on studies of (1) the ternary system CaO-C_5A_3-C_2F, (2) the quaternary system CaO-C_5A_3-C_2F-C_2S, and (3) the quaternary system as modified by 5% magnesia, part II, Am. J. Sci. **244**, 65 (1946).

[10] G. L. Malquori and V. Cirilli, the ferrite phase, Proc. Symposium on Chemistry of Cement, p. 120 (London, 1952).

[11] F. A. Mauer, an analytical balance for recording rapid changes in weight, Rev. Sci. Instr. **26**, 598 (1954).

[12] T. F. Newkirk, Differential thermal analysis above 1200° C, J. Am. Ceram. Soc. **41**, 409 (1958); PCAF Paper 72.

[13] Harold P. Klug and Leroy Alexander, X-ray diffraction procedures for polycrystalline and amorphous materials, p. 716 (John Wiley & Sons, Inc., New York, N. Y., 1954).

[14] R. Roy and E. F. Osborn, The system lithium metasilicate-spodumene-silica, J. Am. Chem. Soc. **71**, 2086 (1949).

[15] G. A. Rankin and F. E. Wright, The ternary system CaO-Al_2O_3-SiO_2, Am. J. Sci. **39**, 1 (1915).

WASHINGTON, July 1958.